6.8-MeV Level

This level is postulated to explain the 1.8- and 6.8-MeV gamma rays of about equal intensity in coincidence at the 1324-keV resonance.

SUMMARY

The decay properties of all intermediate levels observed in this study are summarized in a decay scheme in Fig. 12.

ACKNOWLEDGMENTS

The authors wish to express their appreciation for the assistance of Richard A. Moore, Denny Watson, Carl Peck, Robert Redding, and Urs Wild in machine operation and data analysis. Some of the equipment used was borrowed from the AEC-supported group here. One of us (G. I. H.) did much of the manuscript preparation at the Aeronautical Research Laboratories, Wright-Patterson Air Force Base, Ohio.

PHYSICAL REVIEW VOLUME 128, NUMBER 1 OCTOBER 1, 1962

Elastic Scattering of 6.7-MeV Neutrons from Silver and Indium†

P. R. MALMBERG AND S. C. SNOWDON*
Nucleonics Division, U. S. Naval Research Laboratory, Washington, D. C.
(Received February 13, 1962)

The differential cross sections for the elastic scattering of 6.7-MeV neutrons by silver and indium have been measured over a wide angular range using a standard ring geometry. Improved detection and data treatment techniques were used in an attempt to minimize the errors in the results caused by the contributions from inelastically scattered neutrons. The corrections for finite volume of the scatterer and for double scattering were made using a simplified model that can be treated analytically. The experimental cross sections are, in general, somewhat smaller at the larger scattering angles than the theoretical curves calculated by Bjorklund and Fernbach.

INTRODUCTION

SINCE the proposal of the optical model of the nucleus,[1] many experiments have been performed to verify it and to determine the parameters involved in the various specific choices of the potential. An important class of experiments has been the measurement of the differential cross section for the elastic scattering of neutrons. Early survey experiments[2] emphasized collecting data for a large number of elements at a number of different energies. The present experiment is an attempt to obtain results with better statistical accuracy and less contamination from inelastically scattered neutrons. Measurements were made on silver and indium over a large angular range using 6.7-MeV neutrons.

EXPERIMENT

The neutron source, scatterer, and detector were arranged in a standard ring geometry as may be seen in Fig. 1. The scattering angle θ was varied by using various combinations of source-to-detector distance, ring diameter, and ring position.

Detector counts were taken under three conditions: (a) the arrangement using scatterer as shown in Fig. 1, (b) with scatterer removed to count background, and (c) with both scatterer and attenuator removed to count the direct beam. From these measurements, a "scattering ratio,"

$$S=\frac{\text{scattered counts}-\text{background counts}}{\text{direct counts}-\text{background counts}}, \quad (1)$$

may be computed. An uncorrected differential cross section, σ_A, may be obtained from this scattering ratio by using the expression

$$S=\sigma_A n\int_V Je^{-\sigma nl}dV, \quad (2)$$

where n is the number of atoms per unit volume, σ is the

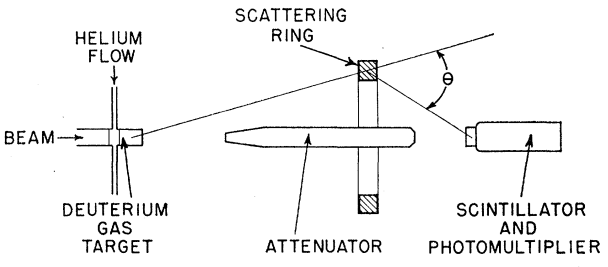

FIG. 1. Experimental arrangement.

† A preliminary report of this work has appeared in Bull. Am. Phys. Soc. 4, 257 (1959).
* Present address: Midwestern Universities Research Association, Madison, Wisconsin.
[1] H. Feshbach, C. E. Porter, and V. F. Weisskopf, Phys. Rev. **96**, 448 (1954).
[2] For example, J. R. Beyster, M. Walt, and E. W. Salmi, Phys. Rev. **104**, 1319 (1956).

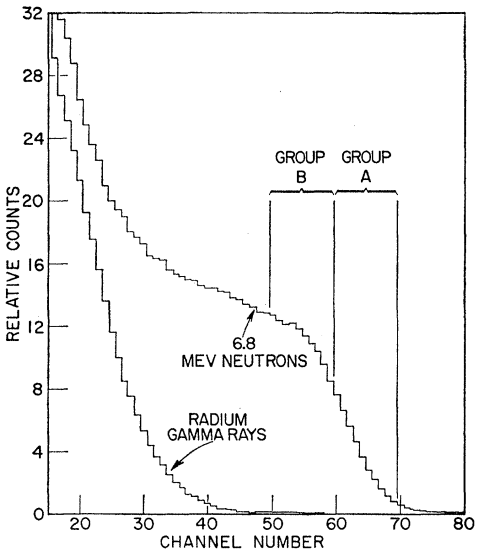

FIG. 2. Typical pulse-height distributions for the detector in a flux of 6.8-MeV neutrons and in a flux of gamma rays. The vertical lines indicate groupings used in data analysis. Group A was used in the final calculations; note the good discrimination against gamma rays for this group. Group B was used in making some estimates of the inelastic scattering contributions to the results calculated from group A.

total cross section, and l is the total length of neutron path inside the sample for each volume element of the integral. The factor J involves distances, angular distribution of source neutrons, and energy and angular sensitivity of the detector. The scattering angle for this cross section is assumed to be that corresponding to the center of the square section of the scatterer.

The neutrons were generated by bombarding a deuterium gas target with a deuteron beam from the NRL 5-MV Van de Graaff accelerator. The target entrance window consisted of two foils of 0.00005-in. nickel separated by 0.06 in. and cooled by a flow of helium gas as shown in Fig. 1.[3] The focused deuteron beam was fanned out by alternating voltages applied across deflector plates to form a rectangular shape somewhat smaller than the size of the foil opening. Typical beam currents were about 8 μA. The 1-in.-long gas target filled to 1 atm pressure produced an average neutron energy before scattering of about 6.7 MeV with a calculated energy spread of 100 keV.

The scatterers, in the shape of rings, were 1 in. square in cross section and had outside diameters of 4, 6, and 8 in. Distances between target and detector ranged between 18 and 80 in.

The neutrons were detected via the knock-on protons in a plastic scintillator.[4] The scintillator was arranged as six small cylinders (0.20-in. diam$\times$0.16 in. high) placed directly on a photomultiplier tube face on a 1-in.-diam circle. These were separated by steel to minimize the chance that a gamma-ray generated electron would penetrate two cylinders and thereby give a pulse of size comparable to those of interest. This modification of a common arrangement[5] has the advantage that it gives a better pulse-height distribution than in the case where the pieces are suspended in a liquid. It was necessary to equalize the response from the separate pieces of scintillator by selective spraying of light-absorbing enamel over parts of the photomultiplier tube face. A typical spectrum from this detector for the direct neutron beam may be seen in Fig. 2. The response to gamma rays also is shown; note the relative absence of large size pulses.

The output from the photomultiplier tube was amplified by a preamplifier and linear amplifier, and then analyzed by a 100-channel pulse-height analyzer. A signal from a mercury-relay pulse generator was fed into the preamplifier in parallel with the photomultiplier output in order to monitor drifts in the electronics. A similar detector was placed near the target for use as a monitor counter. Direct, background, and scattering runs were taken in an interspersed pattern. Scattering or background runs were typically about 20 min long and direct runs one-third as long.

Auxiliary runs were necessary to determine some of the factors that enter into Eq. (2). The angular distribution of the neutrons from the target, the angular sensitivity of the counter, and the dependence of the pulse-height distribution upon neutron energy were measured. The attenuation of the direct beam due to inserting a 1-in.-thick sample of the scattering material in the path was measured in order to calculate the total cross section, σ.

DATA TREATMENT AND RESULTS

It should be expected that part of the neutrons will be scattered inelastically. By using only pulses near the maximum pulse height, the contribution due to the inelastically scattered neutrons can be minimized. The group of pulse heights chosen is indicated as group A in Fig. 2. A measure of the amount of the inelastic neutron contribution can be obtained by comparison with the results of similar calculations performed on the adjacent group B. The range of group A was chosen as a compromise between errors due to possible inelastic contributions, errors due to electronic instabilities, and statistical uncertainties due to the number of counts within the group.

The position of the upper end of pulse-height-distribution curves may vary due to instability of the electronics, and will change for scattered neutrons because a scattered neutron will have less energy than a neutron going directly to the detector. Rather than compensate for these variations in the position by

[3] Similar cooled windows were first reported by R. Nobles, Rev. Sci. Instr. **28**, 962 (1957).

[4] Pilot Scintillator B, Pilot Chemicals, Inc., Watertown, Massachusetts.

[5] J. H. McCrary, H. L. Taylor, and T. W. Bonner, Phys. Rev. **94**, 808(A) (1954); H. L. Taylor, O. Lönsjö, and T. W. Bonner, *ibid.* **100**, 174 (1955).

changing group size and group position for each run, all pulse-height distributions were normalized by scale changes on both channel-number and counts axes so that resultant distributions would be at a standard position relative to the group divisions.[6] This adjustment will be called "end-point" normalization because the actual procedure involved adjustment relative to a point near the upper end of a distribution which was convenient to determine analytically.

The bulk of the numerical treatment of the data including corrections was performed using the NRL digital computer, NAREC. The printed output from the pulse-height analyzer was transcribed onto punched-paper tape in a form suitable to be read into the computer. The data were treated in the following steps to obtain the uncorrected cross sections:

(1) Runs were normalized to a standard number of monitor counts, and a dead-time correction was applied.

(2) Background runs were subtracted from both direct and scattering runs.

(3) Direct and scattering runs were "end point" normalized as described—the direct by compensating for the observed instability, and the scattering by this compensation plus the calculated shifts due to neutron energy changes.

(4) The counts for all the channels within the group were summed.

(5) The scattering ratio, S, was calculated.

(6) From this scattering ratio, the uncorrected cross section, σ_A, was calculated using Eq. (2); the integral being evaluated numerically.

These uncorrected cross sections are plotted in Fig. 3. Results calculated for group B in the same manner are given as a line with data points omitted. The error bars for group B were appreciably smaller, and thus the curves drawn for group B are better defined. For example, the upward inflection near $\cos\theta=-1$ in the silver curve was definitely indicated for group B, but the exact shape for group A is uncertain.

Corrections for finite volume of scatterer and multiple-scattering contributions were omitted in the calculation of these uncorrected cross sections, except for the integral in Eq. (2) involving path length. Although such corrections have been made by Monte Carlo methods,[7] a more convenient and comparably accurate method, considering the statistical uncertainty inherent in Monte Carlo calculations, has been used to correct these data. In this method the double scattering is treated approximately and higher order scatterings are neglected.

The scattering ratio defined by Eq. (1) is made up of contributions due to singly scattered neutrons, (S_1);

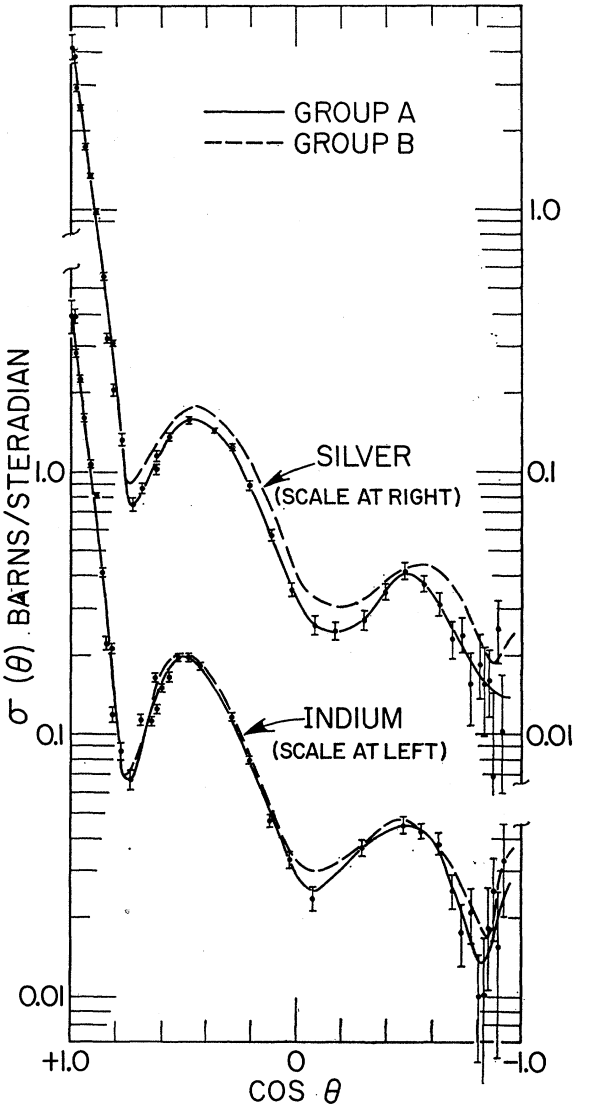

FIG. 3. Uncorrected differential cross sections, σ_A, for silver and indium. Curves drawn for a smooth visual fit of the data points are shown for both group A and group B. Data points are omitted for group B to avoid confusion. Error bars represent counting statistics calculated in an approximate manner. Angle is in laboratory system.

doubly scattered neutrons, (S_2); and higher orders, (S_3,S_4,$\cdots$). If these higher orders are neglected,

$$S=S_1+S_2. \tag{3}$$

The single-scattering contribution is given by the following integral evaluated over the volume of the ring:

$$S_1=\int_V Jn\sigma(\theta)e^{-\sigma n(r_1+r_2)}dV, \tag{4}$$

where $\sigma(\theta)$ is the differential elastic cross section, and r_1 and r_2 are the path lengths of a neutron in the

[6] In this procedure, it is assumed that the relative shape of curves is the same for different energies. This should be adequately correct for the small changes in energy involved (4.4% maximum).

[7] M. Walt and J. R. Beyster, Phys. Rev. **98**, 677 (1955); H. S. Hans and S. C. Snowdon, *ibid.* **108**, 1028 (1957).

scatterer before and after scattering. The factor J is given by

$$J=\epsilon I\gamma(R_0/R_1R_2)^2, \tag{5}$$

where R_0 is the distance between source and detector, R_1 is the distance between source and point of scatter, R_2 is the distance between point of scatter and detector, I is the angular distribution of neutrons from the source relative to the forward direction, ϵ is the angular variation of the counter efficiency relative to the direct path, and γ is the efficiency of the counter for different neutron energies relative to the efficiency for the direct beam.

The double-scattering contribution is given by a double integral,

$$S_2=\int_{V'}\int_{V''} Jn^2\sigma(\theta')\sigma(\theta'') \times\frac{\exp[-\sigma n(r_1'+r_{12}+r_2'')]}{(r_{12})^2}dV'dV'', \tag{6}$$

where the primes refer to the first scatter and the double primes to the second, and where r_{12} is the path length between first and second scattering. The angles θ' and θ'' must combine to give the angle θ of observation.

In order to avoid working with the complex double integral (6), it can be simplified by a number of approximations. It may be noted that, after the first scatter, the distance to the surfaces of the scatterer will be, on the average, about half the length, D, of the side of the square cross section. The major approximation made is therefore that, after the first scatter, the neutron will be located in the center of a sphere of the material of radius $\rho=D/2$. The quantity r_{12} then will be the radial coordinate of this sphere with volume element

$$dV''=r_{12}^2d\Omega''dr_{12}, \tag{7}$$

where $d\Omega''$ is the element of solid angle.

Two less important approximations are also made: that the value of J is determined only by the first scatter, and that the total path length inside the scatterer $(r_1'+r_{12}+r_2'')$ is the same as the path length for single scattering (r_1+r_2). This allows the double volume integral in Eq. (6) to be separated.

Substituting Eq. (7) in Eq. (6), separating the integrals, and integrating dr_{12} from 0 to ρ, the following expression results:

$$S_2=n\left[\int_{V'}Je^{-\sigma nl}dV'\right]\times\left[n\rho\int_{\Omega''}\sigma(\theta')\sigma(\theta'')d\Omega''\right], \tag{8}$$

where $l=r_1+r_2$.

For computational convenience, an approximate differential cross section, σ_A, was defined by Eq. (2). Substituting Eqs. (2), (4), and (8), into Eq. (3) gives the result

$$\sigma_0(\theta)=K[\sigma_A-\sigma_D], \tag{9}$$

where $\sigma_0(\theta)$ is the differential cross section at the angle corresponding to the center of the square section of a scatterer, σ_D is the last bracketed expression in Eq. (8), and K is determined by

$$K\int J\sigma(\theta)e^{-\sigma nl}dV=\sigma_0(\theta)\int Je^{-\sigma nl}dV. \tag{10}$$

It is expected that K is approximately unity except in the regions of the cross section curve that exhibit pronounced curvature.

The Ω'' integral in (8) may be evaluated[8] in terms of a Legendre-polynomial expansion of $\sigma(\theta)$:

$$\sigma(\theta)=\sum_{L=0}^{\infty}A_LP_L(\cos\theta). \tag{11}$$

Substituting this expansion in the Ω'' integral, it may be evaluated[9] to yield the result:

$$\sigma_D=4\pi n\rho\sum_{L=0}^{\infty}\frac{1}{2L+1}A_L^2P_L(\cos\theta). \tag{12}$$

The basic equations used for correcting the data were Eqs. (9), (10), (11), and (12). The integrals were evaluated numerically on the computer. The coefficients of the Legendre-polynomial expansion were calculated using a special matrix[10] that transforms from a set of coordinate values to the expansion coefficients. Twenty-one points (and thus a 21×21 matrix) were used for the fit. It was found that when points evenly spaced in $\cos\theta$ were used the curve calculated using the right-hand side of Eq. (11) did not give a good match to a drawn $\sigma(\theta)$ curve near the ends, although the curve necessarily went through the set of coordinate points chosen. A much better match was obtained using an uneven distribution of points that gave greater weight to the regions near the two ends of the curve.

A method of successive iteration was used to approach the corrected cross section from the experimentally determined uncorrected cross section, σ_A. The method is to use the current approximation of $\sigma_0(\theta)$ to calculate a better K or σ_D, which is then used in the right-hand side of Eq. (9) to calculate a better approximation for $\sigma_0(\theta)$.

The uncorrected cross section, the corrected cross section, and curves for two intermediate steps are given

[8] A general treatment for multiple scattering using Legendre-polynomial expressions is given by S. Goudsmit and J. L. Saunderson, Phys. Rev. **57**, 24 (1940). M. Walt and H. H. Barschall, *ibid.* **93**, 1062 (1954) have used this general method for the correction of neutron scattering data.

[9] W. R. Smythe, *Static and Dynamic Electricity* (McGraw-Hill Book Company, Inc., New York, 1939), pp. 129, 152.

[10] S. C. Snowdon, L. Eisenbud, and J. F. Marshall, J. Appl. Phys. **29**, 950 (1958). The 21×21 C_{kL} matrix used was developed completely by the computer since it was found that eight-place hand-calculated A_{kl} and B_{lL} matrices did not have enough significant figures to generate an accurate C_{kL} matrix.

on Fig. 4 for the case of silver. The data points are not shown, but in each case the correction was applied directly to the data points and a new curve was drawn to fit the new points. The first approximation was the uncorrected cross section, σ_A, (shown as curve A). Curve B shows the result using this σ_A to calculate an improved K but ignoring σ_D, that is $\sigma_D=0$ was assumed. Curve C shows the result following another K calculation and the first double-scattering correction. Curve D shows the result after another K calculation and second double-scattering correction. The process was stopped here although further iterations might have produced some minor deviations from curve D. The difference between uncorrected and corrected cross sections was somewhat smaller for indium,[11] thereby reflecting the fewer atoms per unit volume in this case.

The corrected curves may be integrated to give the total elastic scattering cross section. The results are 2.11 b for silver and 2.08 b for indium (at 6.7 MeV). The measurements of total cross sections gave 4.33 $\pm$0.09 b for silver and 4.39$\pm$0.09 b for indium (at 6.8 MeV) agreeing well with the measurements of Bratenahl, Peterson, and Stoering.[12] In-scattering corrections have been made.

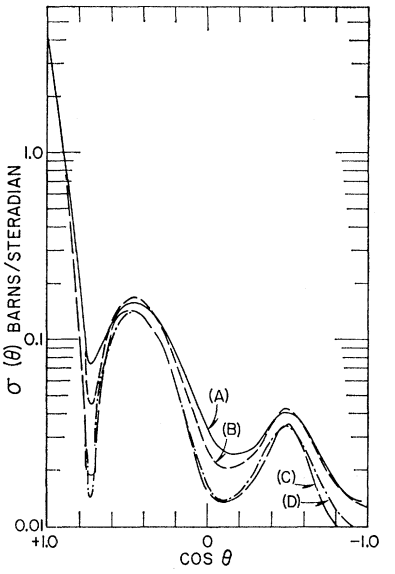

FIG. 4. Correction of cross section data for silver by iteration. Curve A is the uncorrected cross section, σ_A; curve D is the cross section as corrected; and curves B and C represent intermediate steps. (Where curves overlap only one curve is shown.)

ERRORS AND DISCUSSION

Errors can occur in angle, neutron energy, uncorrected differential cross sections, and corrections to the cross sections. In addition, there will remain uncertainties due to inelastic scattering contributions and polarization effects.

Distances were measured to less than $\pm$0.02 in. This could cause a maximum angular error of 1/2° (near 90°).

Under the operating conditions that were used, the energy instability of the deuteron beam is reflected in about a $\pm$0.5% instability in the incident neutron energy. In addition, the energy of the neutrons at the scatterer was not constant since the Van de Graaff potential was not changed from run to run to compensate for the dependence of neutron energy on the angle of emission from the target. This amounted to $\pm$1.2% variation around the 6.7-MeV average neutron energy.

A detailed analysis of the uncertainties in the uncorrected cross-section values would be very difficult as there are a large number of factors that lead to a resultant value and the individual uncertainties in many of these factors will differ for differing data points. Therefore, only the known prominent uncertainties will be considered.

The error bars on the data plotted in Fig. 3 reflect the uncertainties due to counting statistics. Because of the approximations made in these calculations, actual statistical uncertainties would be somewhat greater in the region of good statistics and somewhat less in the region of poor statistics, but this would have little effect on drawing a curve to fit the data.

Group A comprises only a small region at the upper end of the pulse-height spectrum. Therefore, the number of counts that will be within this group will be quite sensitive to how exactly the "end points" for different runs can be normalized to a common value. The short-term "end-point" variations due to either electronic instabilities or changes in energy of the deuteron beam cause the greatest difficulty. Some measurements of these variations indicated that fluctuations of 1/4 channel were common between runs. Based upon this, it would be appropriate to include a corresponding 5% uncertainty for all data points because of these "end-point" uncertainties. At the largest angles, the ratio of background counts to scattered counts is large, which increases the errors due to instability, but the uncertainties due to counting statistics still predominate in this region.

The difference between the corrected and uncorrected data is rather large, so the validity and accuracy of these corrections are important. The corrections for the finite size of the scatterer should not be expected to give correct values in those regions where the curve varies rapidly in the angular range covered by the scatterer. This is especially true in the regions of the

[11] An error was made in the correction procedure in the case of indium. In making the first two K corrections, the curves for silver were used to calculate K instead of the curves for indium. Because of the similarity between the curves for silver and indium, the results of a correction should be similar. As a precaution, however, an additional K correction was made between curves C and D. In a successive iteration method such as this, it is assumed that curves should converge to the correct value independent of minor errors in early stages.

[12] A. Bratenahl, J. M. Peterson, and J. P. Stoering, Phys. Rev. **110**, 927 (1958).

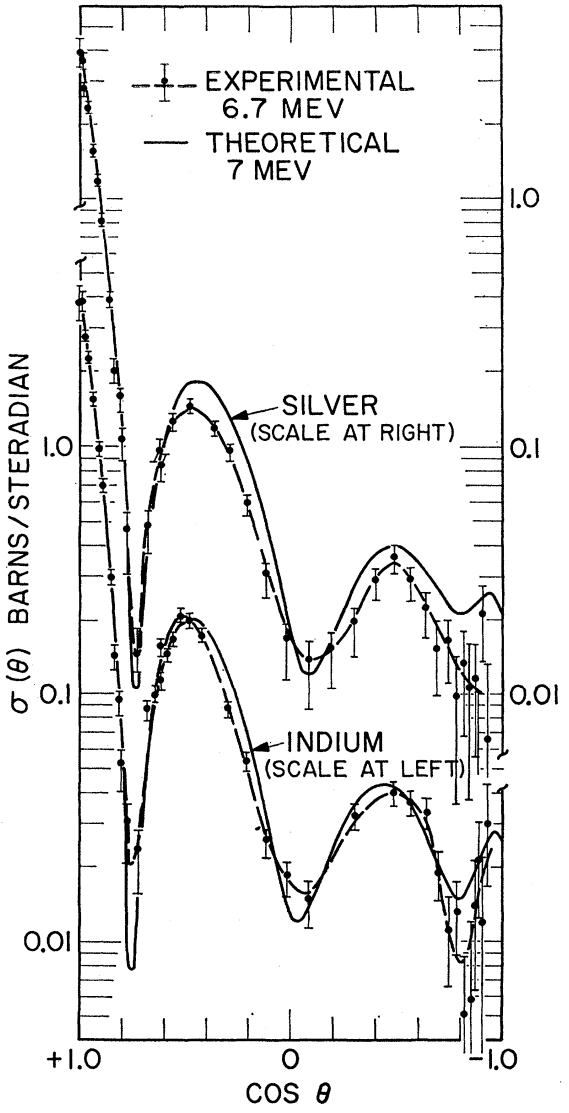

FIG. 5. Differential cross sections for silver and indium, showing the corrected experimental results (for group A) and theoretical curves calculated by Bjorklund and Fernbach (see reference 15) for 7.0 MeV. The error bars represent a combined estimate of the uncertainties as described in the text. The experimental curve is a smooth visual fit to the data.

sharp dips, so corrected points within the deep valleys may have large unknown errors. The double-scattering corrections depend on the validity of the simplified model. In particular, there can be an error in the degree to which the approximately calculated shape of a σ_D curve compares with that of an accurately calculated shape for double scattering. The shape of a σ_D curve calculated from a parent $\sigma(\theta)$ curve is not particularly dependent upon small details of the parent curve. The σ_D curves essentially decrease monotonically with increasing angle and show much less total variation than the parent curve. In this model, the fact has specifically been ignored that many neutrons scattered at about 90° in the first scatter may scatter a second time at any place in the ring, not just in a nearby area. However, a very rough calculation indicates that the contribution, due to these larger-distance double scatterings, should be less than 1 mb/sr at any angle. In addition, an error in general magnitude of the double-scattering correction would result from an incorrect choice of sphere radius for the model. A 20–30% uncertainty in the double-scattering corrections would not be unreasonable. It is because of this large uncertainty, that the higher-order scatterings (calculable on extension of the model) which would be about the size of the uncertainty itself were neglected.

Only a finite number of successive iterations were made in performing the corrections, but the curves do seem to be converging to a final curve. Considering the other uncertainties, the error due to termination of iterations appears to be negligible.

It is difficult to estimate the contribution due to inelastic scattering. The difference between the uncorrected cross sections (see Fig. 3) for group B and group A averages about 8 mb/sr for silver at angles greater than 90° and about 3 mb/sr for indium. The contribution of the inelastic neutrons to group A should be less than the difference between A and B, and might be guessed as not greater than 4 mb/sr for silver and 2 mb/sr for indium. Silver might be expected to give more inelastically scattered neutrons in the energy range of detection since the low-lying levels of indium involve large spin changes from the ground state, and at least one level in each silver isotope does not.[13]

The polarization present in the neutrons emitted from the target will cause an uncertainty in the results. A calculated value of polarization for the largest angle of neutron emission in the present experiment is 2.6%.[14] This would cause a comparable "error" in the measured points in angular regions in which the asymmetry produced in a scattering itself is large.

It is difficult to deal with these several sources of uncertainty in a satisfactory analytic manner, but it still appeared desirable to indicate a combined uncertainty for the corrected experimental data which are presented in Fig. 5. These combined uncertainties were calculated assuming that errors were independent and that positive and negative error contributions could be combined separately. The three positive contributions included were statistical uncertainties, uncertainties due to electronics instability, and a 10% uncertainty in the double-scattering correction. The four negative contributions included were statistical uncertainties, uncertainties due to electronics instability, estimates of inelastic scattering contributions, and a 30% uncertainty

[13] *Nuclear Data Sheets*, National Academy of Sciences, National Research Council, (U. S. Government Printing Office, Washington, D. C.), NRC 58-5-41, 60-2-49, 60-2-100, and 60-3-105.

[14] This value is based on a curve presented by W. W. Daehnick, Phys. Rev. **115**, 1008 (1959). The angular dependence of polarization was assumed to be proportional to $(\sin 2\theta)/\sigma(\theta)$ for the deuteron energy used in the present experiment.

in the double-scattering correction. The two different values for the uncertainty in the double-scattering correction were based on a feeling that the amount of this correction was most likely underestimated.

Theoretical curves calculated by Bjorklund and Fernbach[15] are also presented in Fig. 5. The calculations are for an optical-model potential having a real central well with rounded edges and surface absorption and spin-orbit terms. These calculations give the shape-elastic scattering only and would be expected to give values lower than the experimental values which include the compound-elastic scattering. The slight energy difference between the theoretical and experimental curves should not significantly affect a comparison of the two.

The data points for indium could almost fit the theoretical curve within counting statistics except for the high side of the peak near $\cos\theta=1/2$, although the fit at the large angles would be marginal. The silver data do not show as good an agreement, being lower than the theoretical curve over a much larger range of the whole curve. It is not likely that the difference in the agreement between silver and indium is due to experimental and calculational procedures since these were essentially identical for the two elements.

The theoretical fits were based upon a large variety of experimental data. The 7-MeV calculations were based in part upon data in which inelastically scattered neutrons with more than 80% of the energy of elastically scattered neutrons might have been counted. This could have resulted in an appreciably larger inelastic scattering contribution than in the case of the present experiment where the effective bias was set at about the 90% level.

[15] F. Bjorklund and S. Fernbach, University of California Radiation Laboratory Report, UCRL-4927-T, 1957 (unpublished); also Phys. Rev. **109**, 1295 (1958).

ACKNOWLEDGMENTS

The authors wish to express thanks to Dr. R. O. Bondelid and Dr. E. A. Wolicki, who assisted in the early stages of the experiment; to Mrs. Josephine Eves, who transcribed the printed pulse-height data records onto punched-paper tape; to the staff of the NAREC for their suggestions on computer programming for the data treatment; and to S. Chappell, who checked some of the hand calculations.

PHYSICAL REVIEW VOLUME 128, NUMBER 1 OCTOBER 1, 1962

Some Gamma-Ray Cascades in Rh^{103}, Ce^{140}, and Dy^{160}†

S. I. H. NAQVI* AND B. G. HOGG
Allen Physics Laboratory, The University of Manitoba, Winnipeg, Canada
(Received October 27, 1961; revised manuscript received June 20, 1962)

The 445–53 keV cascade in Rh^{103} was found to have an intensity <0.5 relative to 1000 for the intensity of the most intense, 498-keV, gamma ray in the decay scheme. No evidence was found for a 323-keV gamma ray in this scheme. Spins of 5/2 for the 538-keV level and 7/2 for the 650-keV level in Rh^{103} are assigned in keeping with the relative intensities of <0.5 and 4 for the 445- and 538-keV gamma rays, respectively. Cascades of 1088–814, 1415–487, and 1596–306 keV have been observed in Ce^{140} and a level at 3498 keV introduced into the scheme. The beta feed to this level is estimated to be $\sim 0.002\%$ of the most intense beta group in the decay of La^{140}. Cascades of 87–1312 and 197–1200 have been observed in Dy^{160} and a level at 1484 keV is introduced.

INTRODUCTION

MANY cases of nuclear de-excitation occur through a series of cascades to the ground state. The total energy involved in the various cascades between two given levels is, of course, the same.

A sum-coincidence spectrometer[1] is particularly useful in studying weak gamma-ray cascades, especially in cases where the decay is complex. The spectrum that one obtains for a two-gamma cascade is uncluttered by Compton edges and gamma rays from the other transitions in the decay. The spectrum shows prominently only the sum peak and the two gamma rays of the cascade.

In these experiments sources of Ru^{103}, La^{140}, and Tb^{160} of ~ 5 μC strength each were used to investigate a number of cascades from excited states of Rh^{103}, Ce^{140}, and Dy^{160}, respectively.

APPARATUS AND METHOD[2]

A block diagram of the apparatus is shown in Fig. 1. The two NaI(Tl) detectors are Harshaw "Integral Line" detector type 6S4/2 (1.5- × 1-in. crystal coupled to a 2-in. photomultiplier tube). Occasionally and with-

† Supported by the Defense Research Board of Canada and the National Research Council of Canada.
* Now at St. Paul's College, The University of Manitoba, Winnipeg, Canada.
[1] A. M. Hoogenboom, Nuclear Instr. **3**, 57 (1958).

[2] S. I. H. Naqvi, Nuclear Instr. (to be published).